

Electrochemical Synthesis and Corrosion Protection Properties of Poly(*o*-toluidine) Coatings on Low Carbon Steel

Vandana Shinde,¹ S. R. Sainkar,² P. P. Patil¹

¹Department of Physics, North Maharashtra University, Jalgaon 425 001, Maharashtra, India

²National Chemical Laboratory, Pune 411 008, India

Received 4 November 2003; accepted 4 June 2004

DOI 10.1002/app.21497

Published online in Wiley InterScience (www.interscience.wiley.com).

ABSTRACT: Uniform and strongly adherent poly(*o*-toluidine) (POT) coatings have been synthesized on low carbon steel (LCS) substrates by electrochemical polymerization (ECP) of *o*-toluidine under cyclic voltammetric conditions from an aqueous sodium tartrate solution. Cyclic voltammetry (CV), UV-visible absorption spectroscopy, Fourier transform infrared spectroscopy (FTIR), X-ray diffraction (XRD) measurements, and scanning electron microscopy (SEM) were used to characterize these coatings, which indicates that the sodium tartrate is a suitable medium for the ECP of *o*-toluidine and it occurs without noticeable dissolution of LCS. Corrosion protection properties of the POT coatings

were evaluated in aqueous 3% NaCl by the potentiodynamic polarization measurements and CV. The result of the potentiodynamic polarization demonstrates that the POT coating has ability to protect the LCS against corrosion. The corrosion potential was about 334 mV more positive in aqueous 3% NaCl for the POT-coated LCS than that of bare LCS and reduces the corrosion rate of LCS almost by a factor of 50. © 2005 Wiley Periodicals, Inc. *J Appl Polym Sci* 96: 685–695, 2005

Key words: corrosion resistant coatings; conducting polymers; poly(*o*-toluidine); FT-IR; UV-vis spectroscopy; electrochemical polymerization; cyclic voltammetry

INTRODUCTION

During the last decade, the conducting polymers have received focused attention in many technological areas such as rechargeable batteries, sensors, electromagnetic interference (EMI) shielding, electrochromic display devices, smart windows, molecular devices, energy storage systems, membrane gas separation, etc. due to their remarkable physical attributes.^{1–6} One of the most important applications of these materials that is attracting considerable attention is in corrosion protection of metals. The conducting polymer must be in the coating form and it should be strongly adherent to the metal surface so far as corrosion protection is concerned.

The electrochemical polymerization (ECP) is a simple, relatively inexpensive, and most convenient route for the synthesis of such a coating structures.^{1,2} The most salient feature of this route is that the process of polymerization and the coating formation takes place simultaneously. Although the conducting polymers are found to be the most promising materials for corrosion protection, the ECP of conducting polymers is not easy on oxidizable metals. A number of reports on

the synthesis and characterization of conducting polymer coatings on oxidizable metals such as iron, aluminum, zinc, etc. have appeared in the literature during the past 3–4 years.^{7–10} The common feature of these studies is that the synthesis of conducting polymer coatings on oxidizable metals is preceded by the dissolution of the base metal at a potential lower than the oxidation potential of the monomer. Thus, the oxidation of the metal appears as a simultaneous and competitive oxidation process at the potentials adequate for the formation of the polymer. A successful ECP of conducting polymer on oxidizable metals demands careful choice of the solvent, supporting electrolyte and the establishment of electrochemical parameters that will strongly passivate the metal without impeding the electropolymerization process.

The possibility of using polyaniline (PANI) coating for corrosion protection of metals was first reported by DeBerry et al.¹¹ It was further proved that the PANI has the ability to serve as a corrosion protective coating on metals in both acidic and neutral solutions. Polypyrrole (PPY) has also been investigated as a possible coating for corrosion protection.¹² However, the main disadvantage of PPY is that the non-aqueous bath is usually required for its deposition. The incorporation of constituents in the polymer skeleton is a common technique to synthesize polymers having improved properties.^{13,14} This concept has been successfully applied to PANI. Considerable work is still

Correspondence to: P. P. Patil (pnmu@yahoo.co.in).

needed to understand the basic issues related to the ECP of substituted anilines on oxidizable metals and to explore the possibility of utilizing them as an alternative to PANI for corrosion protection.

Recently, our group has investigated the ECP of *o*-anisidine in aqueous oxalic acid solution on LCS substrates using cyclic voltammetry.¹⁵ It has been shown that the oxalic acid is a suitable medium for the ECP of OA on the LCS substrate and it favors the formation of the ES phase of POA. However, these coatings were not able to protect the LCS substrates from corrosion.

In the studies reported in this article, an attempt has been made to synthesize the POT coatings on LCS by ECP of *o*-toluidine under cyclic voltammetric conditions from aqueous sodium tartrate solution and to investigate the corrosion protection properties of these coatings in a chloride environment. The objectives of the present study are i) to study the ECP of *o*-toluidine to generate strongly adherent POT coatings on LCS substrates from aqueous sodium tartrate solution; ii) to identify the oxidation state of POT synthesized from sodium tartrate medium on LCS substrates, and iii) to examine the possibility of using the POT coatings for corrosion protection of LCS in a chloride environment. The reasons for selecting the *o*-toluidine monomer are many and obvious. These reasons are i) The monomer *o*-toluidine is commercially available at low cost, ii) the conversion of monomer to polymer is a straightforward process, and iii) the *o*-toluidine is a substituted derivative of aniline with a methyl ($-\text{CH}_3$) group substituted at the *ortho*-position. This study, therefore, explores the possibility of utilizing the POT as an alternative to PANI for corrosion protection of LCS.

This study has clearly indicated that the ECP of *o*-toluidine in sodium tartrate solution results in the deposition of uniform and strongly adherent POT coatings on LCS substrates. The POT coating exhibits excellent corrosion protection properties and is found to be the most promising coating material for corrosion protection of LCS in aqueous 3% NaCl.

EXPERIMENTAL PROCEDURES

The POT coatings were synthesized by ECP of *o*-toluidine on LCS substrates under cyclic voltammetric conditions. In the present study, the aqueous solution of sodium tartrate was used as the supporting electrolyte. The *o*-toluidine monomer was double distilled prior to its use. The concentrations of sodium tartrate and *o*-toluidine were kept constant at 0.1M and 0.1M, respectively. The ECP was carried out in a single-compartment three-electrode cell with LCS as the working electrode (1.5 cm²), platinum as the counter-electrode, and saturated calomel electrode (SCE) as the reference electrode. The cyclic voltammetric condi-

tions were maintained using a SI 1280B Solartron Electrochemical Measurement System (U.K.) controlled by corrosion software (CorrWare, Electrochemistry/Corrosion Software, Scribner Associates Inc. supplied by Solartron, U.K.). The synthesis was carried out by cycling continuously the electrode potential between -500 and $1,500$ mV at a potential scan rate of 20 mV/s. The number of cycles was varied from 1 to 25. After deposition the working electrode was removed from the electrolyte and rinsed with double distilled water and dried in air.

The corrosion studies were performed at room temperature in aqueous solution of 3% NaCl by using the potentiodynamic polarization technique and CV. For these measurements, a Teflon holder was used to encase the POT-coated LCS substrates so as to leave an area of ~ 0.4 cm² exposed to the solution. The polarization resistance measurements were performed by sweeping the potential between -250 and 250 mV from the open circuit potential (OCP) at a scan rate of 2 mV/s. Before polarization the substrates were immersed into the solution and the OCP was monitored until a constant value was reached. The corrosion potential (E_{corr}) and corrosion current density (I_{corr}) were obtained from the slopes of linear polarization curves. The corrosion rate (CR) was calculated by using the following expression:¹⁶

$$\text{CR}(\text{mm}/\text{y}) = 3.268 \times 10^3 \frac{I_{\text{corr}} \text{EW}}{\rho}$$

where I_{corr} is corrosion current density (A/cm²), EW is equivalent weight of LCS (g) and ρ is the density of LCS (g/cm³).

All the measurements were repeated at least four times and good reproducibility of the results was observed. The ability of the POT coating to protect the LCS against dissolution was studied by recording the cyclic voltammograms in an aqueous solution of 0.1M sodium tartrate (without *o*-toluidine monomer) in the potential range between -500 and $1,500$ mV at a scan rate of 20 mV/s.

The FTIR transmission spectrum of POT coating was recorded in horizontally attenuated total reflectance (HATR) mode in the spectral range 4000–400 cm⁻¹ using a Perkin–Elmer spectrometer, SPECTRUM 2000 Series II, USA. The optical absorption studies of these coatings were carried out *ex situ* at room temperature in the wavelength range 300–1100 nm using a microprocessor controlled double beam UV-visible spectrophotometer (Hitachi, Model U 2000). The structural properties were investigated using XRD. The X-ray diffractograms were recorded with a Rigaku diffractometer (Miniflex Model, Rigaku, Japan) having Cu K α ($\lambda = 1.542$ Å). SEM was employed to characterize the surface morphology with a Leica Cambridge 440 Microscope (UK).

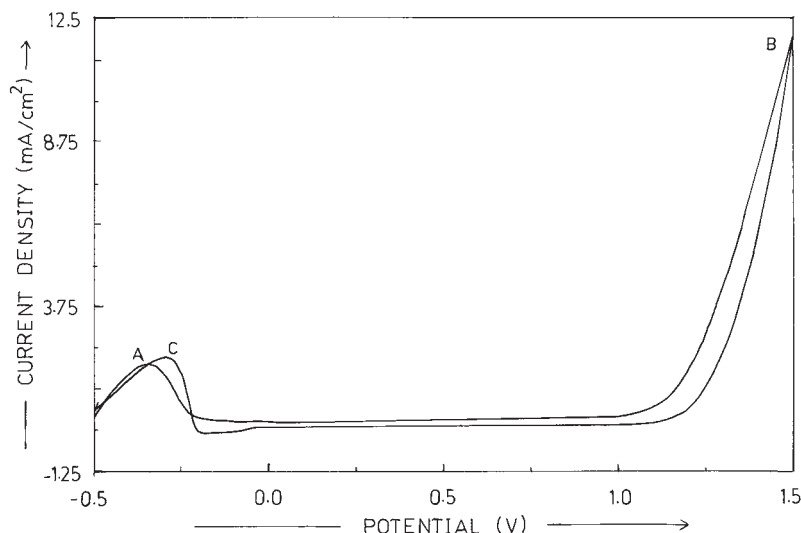


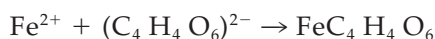
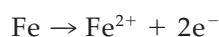
Figure 1 Cyclic voltammogram recorded during the polarization of LCS electrode in 0.1M sodium tartrate solution. Scan rate: 20 mV/s.

RESULTS AND DISCUSSION

Electrochemical behavior of LCS in an aqueous sodium tartrate solution

To understand the different processes occurring at the LCS electrode surface, the LCS electrodes were first polarized in 0.1M aqueous sodium tartrate solution by cycling continuously the electrode potential between -500 and $1,500$ mV at a potential scan rate of 20 mV/s. The corresponding first scan of the voltammetric response of the LCS electrode is shown in Figure 1. The first positive cycle is characterized by i) an anodic peak (A) at -345 mV; ii) negligibly small oxidation current between -207 and $1,114$ mV; and iii) onset of an oxidation wave (B) at $\sim 1,114$ mV and beyond this potential high anodic current flows. The anodic current decays very sharply and a negligibly small current is seen until -206 mV. The negative cycle terminates with an oxidation peak (C) at approximately -301 mV.

The anodic peak A is attributed to the dissolution of the LCS electrode surface, which produces Fe^{2+} ions in its vicinity. These ions interact with the tartrate counter-ions of the electrolyte to form insoluble iron(II) tartrate ($\text{FeC}_4\text{H}_4\text{O}_6$), which adheres to the electrode surface, thereby forming an iron tartrate film.¹⁷ This interphase is produced according to the following two reactions:



The observation of negligibly small anodic current densities in the potential range -207 to $1,114$ mV

indicates the passivation of the LCS electrode surface via the formation of the iron tartrate interphase. The iron tartrate film inhibits the dissolution of the electrode surface and, as a result, just after the peak A, the current density decreases and attains a negligibly small value.

The oxidation wave B is attributed to the oxidation of the electrolyte. During reverse scan, an anodic peak C appears at approximately -301 mV, which is attributed to the reactivation of the LCS electrode surface during the negative cycle. The similar behavior of iron electrode polarized in an oxalic acid was observed by Mengoli and Musiani¹⁸ and Beck et al.¹² They have attributed this peak to a new oxidation accompanied by the rebuilding of the FeC_2O_4 layer. By analogy, the anodic peak C observed during the negative cycle is attributed to a similar process leading to the reconstruction of $\text{FeC}_4\text{H}_4\text{O}_6$ layer on the electrode surface.

On repetitive cycling, the voltammograms identical to that of first scan are obtained and it is observed that the current density corresponding to the peak A increases with the number of scans. This suggests that a continuous dissolution of the LCS electrode occurs and consequently the electrode surface is not passivated even after 20 scans.

To understand the observed CV results, we have performed the XRD measurements of the LCS electrode polarized in 0.1M sodium tartrate solution. The XRD pattern [Fig.2(a)] of bare LCS substrate shows a characteristic diffraction peak at an angle of 44.82° , indicating its polycrystalline nature. The XRD pattern of the LCS electrode polarized in 0.1M sodium tartrate solution is shown in Fig.2(b). Apart from the characteristic peak of LCS, the XRD pattern indicates the presence of diffraction peaks at angles of 36.60° and

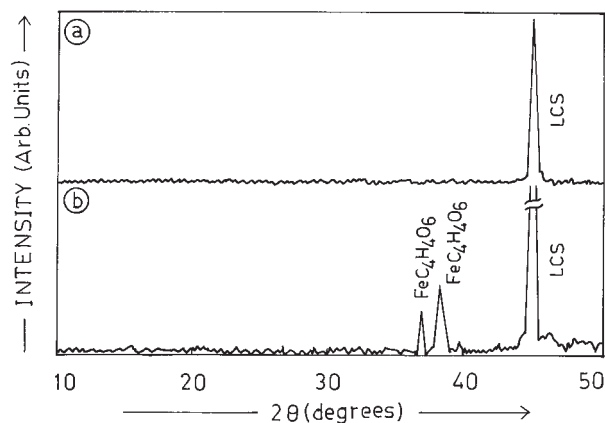


Figure 2 XRD pattern of (a) bare LCS and (b) LCS substrate polarized in 0.1M sodium tartrate solution.

38.0° due to the iron tartrate interphase. Thus, the XRD result clearly reveals the formation of the iron tartrate on the LCS electrode surface. However, the CV results indicate a continuous dissolution of the LCS electrode even after 20 cycles. It seems that, under the experimental conditions employed in the present study, the complete coverage of the LCS electrode surface with the iron tartrate interphase is not achieved in 25 cycles and, as a consequence, the dissolution of the electrode surface is not inhibited. It can be argued that the iron tartrate interphase may be deposited randomly on the substrate surface and, as a result, some area of the bare LCS remains uncovered.

To support this argument, we have characterized the LCS electrode polarized in a 0.1M sodium tartrate solution by SEM. The area of the electrode surface is scanned while recording the SEM images and the corresponding results are shown in Figure 3. It was observed that the electrode surface is nonuniform and it clearly indicates the two types of regions. The SEM images of these regions are drastically different from each other. The SEM image of the first region [Fig.3(a)] reveals the deposition of a thin layer of ill-defined structure. The surface morphology of the second region [Fig.3(b)] does not indicate any deposition at the surface of the LCS electrode. This result confirms that the LCS electrode surface is not completely covered with the passive iron tartrate layer and supports the CV and XRD results.

The observation of the anodic peak A in all scans reveals that, under the experimental conditions employed in this study, less efficient passivation of the LCS electrode surface takes place and as a result it remains active throughout the experiment. As a consequence, the dissolution of the electrode surface is not inhibited. Thus, the polarization of the LCS electrode in 0.1M aqueous sodium tartrate solution does not lead into the passivation of the electrode surface.

Electrochemical polymerization of *o*-toluidine on LCS from aqueous sodium tartrate solution

The first, second, and tenth scans of the CV recorded during the ECP of *o*-toluidine on the LCS electrode from 0.1M sodium tartrate solution are shown in Figure 4. The first positive cycle is characterized by a negligibly small anodic peak A at approximately -404 mV and oxidation wave (B) at ~ 922 mV. The anodic peak A is similar to that observed without *o*-toluidine. However, the observation of the negligibly small current density corresponding to the peak A clearly indicates that the dissolution of the LCS substrate is insignificant in the presence of *o*-toluidine. Moreover, the current densities corresponding to the different peaks in the voltammogram decrease significantly when *o*-toluidine is in the solution, which indicates that the *o*-toluidine is involved in the passivation process. The oxidation wave B at ~ 922 mV is attributed to the oxidation of *o*-toluidine since a brownish-black colored uniform film is deposited on the LCS substrate. It is important to stress that the *o*-toluidine oxidation occurs at ~ 922 mV, suggesting that the electrochemical polymerization may occur without oxidizing the tartrate counterions in the electrolyte. The absence of the peak C during the negative cycle may be attributed to the stabilization of the LCS electrode surface due to formation of an adherent POT coating.

During the next scan, the peak A is not observed, however, the rest of the features are similar to that of the first scan. This suggests that, in the presence of *o*-toluidine, the aqueous sodium tartrate medium efficiently protects the LCS substrate against dissolution and probably this may be due to the efficient passivation of the steel surface via the formation of iron tartrate interphase. On repetitive cycling, voltammograms identical to that of the second scan are obtained. The coverage of the LCS surface by POT appears to inhibit the dissolution of the electrode. Also, the current density corresponding to the oxidation wave B decreases gradually with the number of scans. This may be attributed to the formation of electroinactive POT coating. The visualization of the LCS electrode after 20 scans reveals the formation of strongly adherent brownish-black colored POT coating.

The FTIR spectrum of POT coating synthesized on LCS under cyclic voltammetric conditions (10 cycles) recorded in HATR mode is shown in Figure 5. This spectrum exhibits the following spectral features:^{19,20} i) A broad band at ~ 3449 cm⁻¹ due to the characteristic N-H stretching vibration suggests the presence of -NH- groups in *o*-toluidine units. ii) The band at ~ 2930 cm⁻¹ is associated with C-H stretching in the methylene group. iii) The band at ~ 1646 cm⁻¹ is indicative of stretching vibrations in quinoid (Q) rings.¹⁹⁻²¹ iv) The band ~ 1458 cm⁻¹ represents the stretching vibrations of the benzoid (B) rings.¹⁹⁻²¹ v)

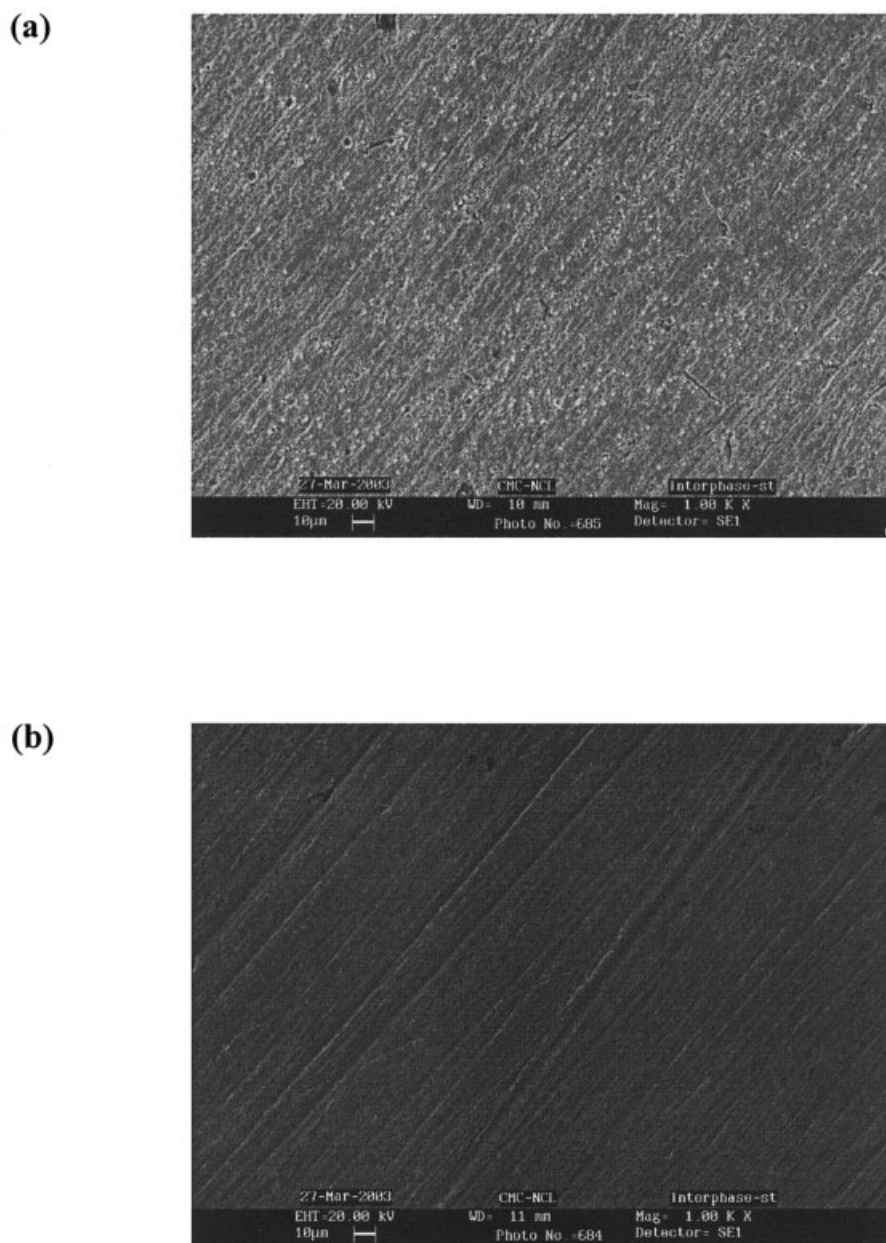
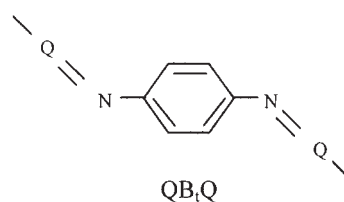


Figure 3 SEM image of the LCS substrates polarized in 0.1M sodium tartrate solution.

The presence of Q and B bands clearly show that the POT coating is composed of amine and imine units. It is known that the ideal form of PANI contains roughly equal amounts of Q and B units. The relative intensity (1646/1458) of these bands is greater than unity. Therefore, it can be concluded that the formation of PB is predominant in the coating.¹⁹⁻²¹ vi) The bands at 1722 and 1278 cm^{-1} are attributed to the presence of carboxylic groups of sodium tartrate in the POT coating. The presence of these strong bands reflects the formation of the oxidized form of POT. vii) The presence of the C–N stretching band at $\sim 1378 \text{ cm}^{-1}$ is consistent with the results reported by Tang et al.,¹⁹ who have also observed the similar bands for POT.

The band at $\sim 1378 \text{ cm}^{-1}$ is assigned to the C–N stretching in QB_tQ environment, where B_t represents a *trans*-benzoid unit:



(viii) The bands at 1122 and 1071 cm^{-1} are attributed to the 1–4 substitution on the benzene ring. (ix) The

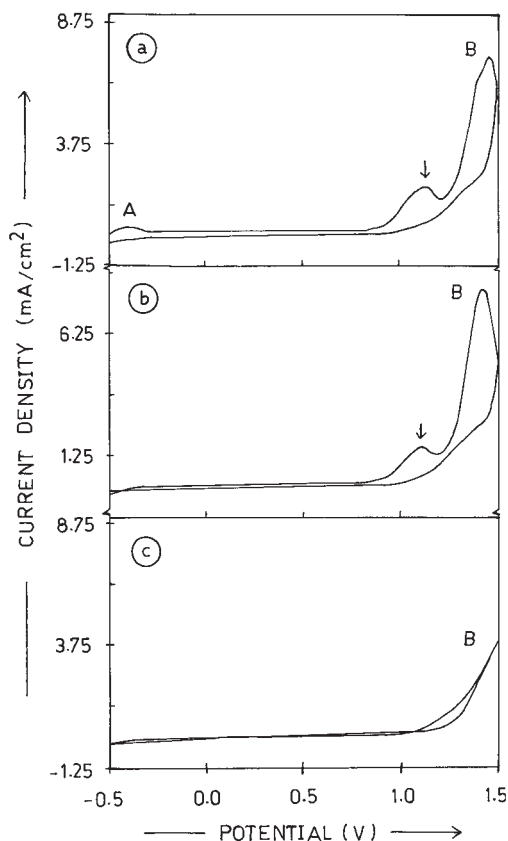


Figure 4 Cyclic voltammogram scans (a) first, (b) second, and (c) tenth recorded during the synthesis of POT coating on LCS substrate under cyclic voltammetric conditions. Scan rate : 20 mV/s.

observation of the bands between 800 and 700 cm^{-1} reveals the occurrence of the 1-3 substitutions. Thus, the FTIR spectroscopic study indicates that the ECP of

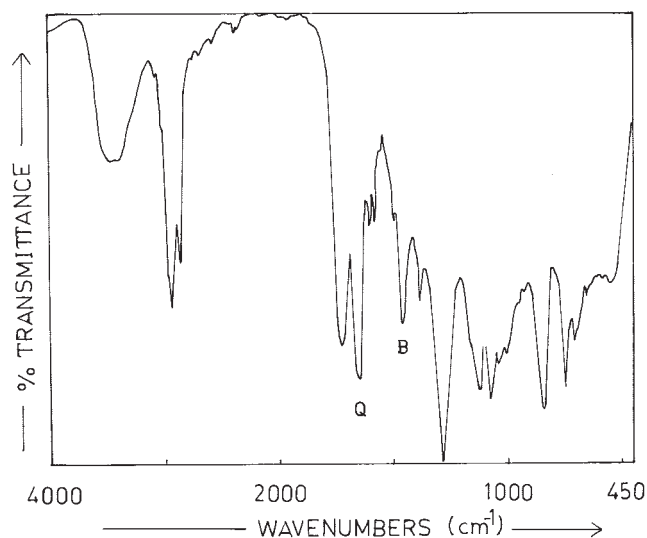


Figure 5 FTIR spectrum of the POT coating synthesized on LCS substrate under cyclic voltammetric conditions.

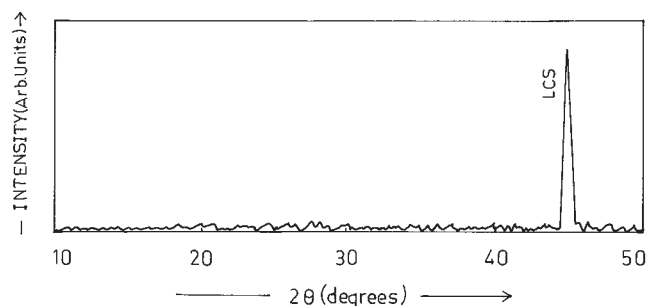


Figure 6 XRD pattern of the POT coating synthesized on LCS substrate under cyclic voltammetric conditions.

o-toluidine has occurred and results in the formation of the oxidized form of POT on the electrode surface.

The XRD pattern of the POT coating synthesized with 25 scans (Fig.6) exhibits only one diffraction peak corresponding to LCS. It is surprising to observe that the XRD pattern does not show the diffraction peaks corresponding to iron tartrate interphase. Also, as the POT coating has a highly disordered structure, it does not indicate any diffraction peak. Thus, the XRD result reveals that the iron tartrate interphase does not exist at the electrode surface.

Very recently, we have investigated the ECP of *o*-toluidine on LCS substrates from the aqueous oxalic acid solution.²² It has been shown that the formation of the passive iron oxalate interphase and its subsequent decomposition is necessary for the ECP of *o*-toluidine to occur on the LCS substrates. By analogy, it may be argued that the iron tartrate layer formed during early stages decomposes and facilitates the ECP of *o*-toluidine on LCS.

The SEM image of the POT coating synthesized on LCS (25 cycles) is shown in Figure 7. It clearly reveals that the POT coating is relatively uniform, compact, and featureless.

To identify the formation and deposition of the different oxidation forms of POT with variation in the coating thickness, we have synthesized the coatings by 1, 5, and 25 scans and performed the optical absorption spectroscopy study. The corresponding optical absorption spectra are shown in Figure 8. It is clearly seen that these spectra exhibit systematic changes in peak positions and relative intensities with variation in the number of scans. The optical absorption spectrum of POT coating deposited with 25 scans is completely different in all respects with the spectrum of the POT coating deposited with only a single scan. The increase in the overall absorbance with the increase in the number of scans used for the synthesis indicates the increase in the thickness of the coating with the number of scans.

The optical absorption spectrum of POT coating deposited with only a single scan [Fig.8(a)] shows a well-defined peak at $\sim 740\text{ nm}$ and it is attributed to

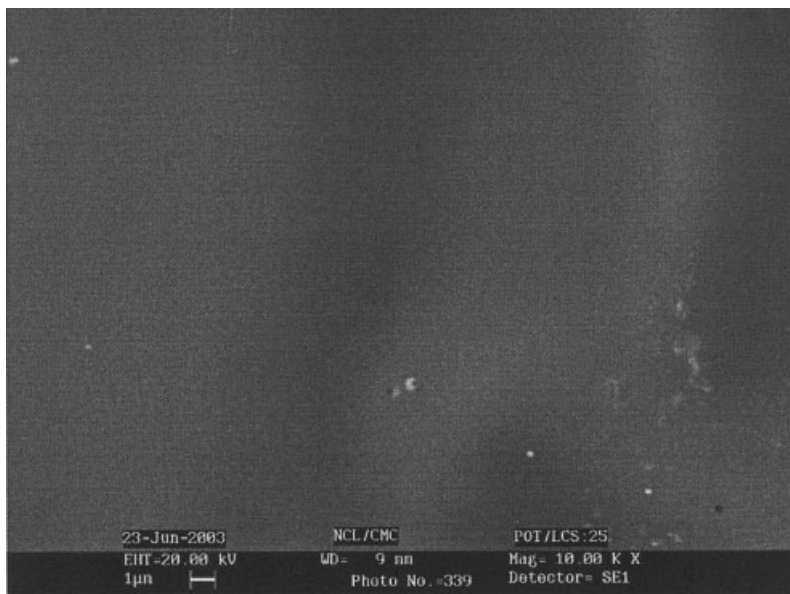


Figure 7 SEM image of POT coating synthesized on LCS substrate under cyclic voltammetric conditions.

the formation of the ES phase of POT, which is the only electrically conducting phase of POT.²³ When the coating was synthesized by 5 scans, the optical absorption spectrum [Fig.8(b)] exhibited a noticeable difference compared with Figure 8(a). First, it indicates an increase in the intensity of the peak at ~ 750 nm. Second, it shows an emergence of the shoulder at

~ 540 nm. The shoulder at ~ 540 nm is the signature of the formation of the PB phase of POT.²³ The PB is the fully oxidized form of POT and it is insulating in nature. The simultaneous appearance of the 750 nm peak and the shoulder at 540 nm clearly reveals the formation of the mixed phase of PB and the ES form of POT. The optical absorption spectrum of POT coating deposited with 25 scans [Fig.8(c)] reveals the exclusive formation of the PB form of POT.

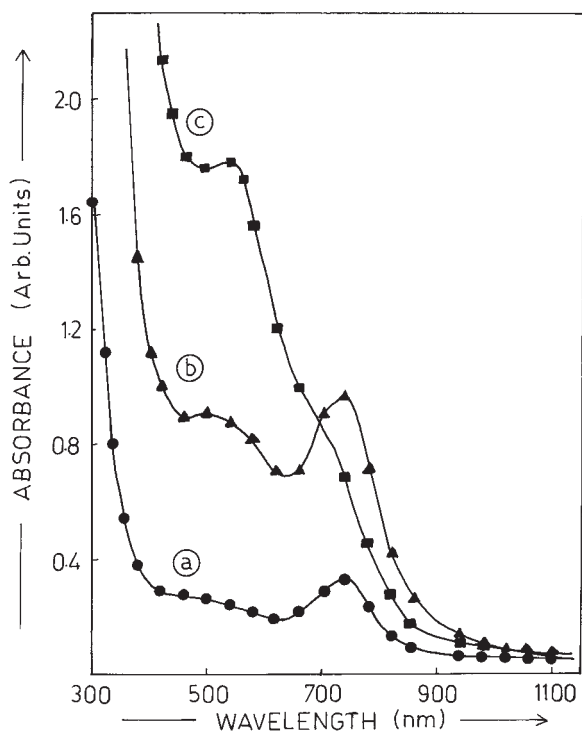


Figure 8 Optical absorption spectrum of POT coating synthesized by (a) 1, (b) 5, and (c) 25 scans in DMSO solution.

The results of the present study clearly show that aqueous sodium tartrate solution is a suitable medium for the ECP of *o*-toluidine on the LCS substrate. The most striking feature is that the ECP of *o*-toluidine occurs without noticeable dissolution of LCS. The tartrate ions are playing a twofold role: i) they act as a passivating agents of the LCS surface as the electrochemical polymerization proceeds and ii) they are incorporated into POT as dopants.

Corrosion protection properties of the POT coating

The potentiodynamic polarization curves for bare LCS and POT coated LCS (25 cycles) in aqueous solution of 3% NaCl are shown in Figure 9. The values of the corrosion potentials, corrosion current densities, and corrosion rates obtained from these curves are given in Table I. It is seen that the values of corrosion potential (E_{corr}) and corrosion current density (I_{corr}) are far lower than the corresponding values for bare LCS, indicating the corrosion-resistant feature of the coating. The I_{corr} decreases from $30.72 \mu\text{A}/\text{cm}^2$ for bare LCS to $0.65 \mu\text{A}/\text{cm}^2$ for POT coated LCS. The E_{corr} increases from -710 mV for bare LCS to -376 mV for POT coated LCS. The positive shift of 334 mV in E_{corr}

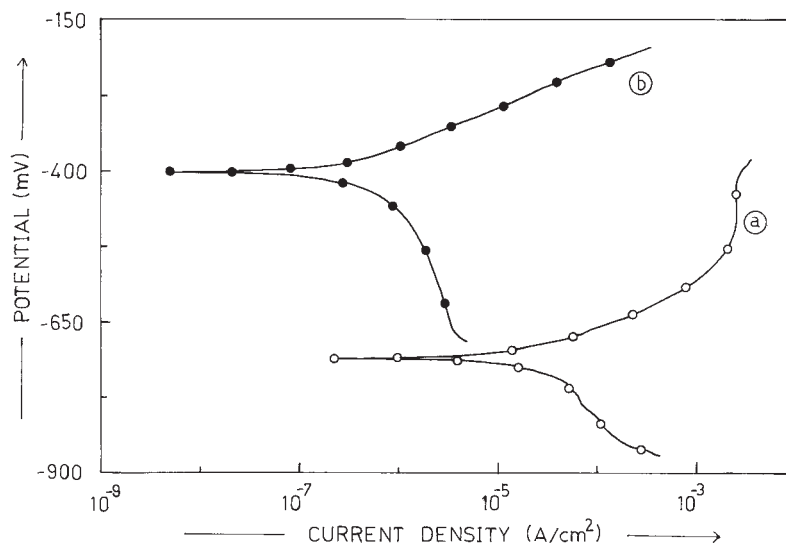


Figure 9 Potentiodynamic polarization curves for (a) bare LCS and (b) POT coated on LCS in aqueous 3% NaCl solution.

indicates the protection of the LCS surface by the POT coating. The corrosion rate of LCS is significantly reduced as a result of the reduction in the I_{corr} . The corrosion rate of LCS is found to be ~ 0.007 mm/y which is ~ 50 times lower than that observed for bare LCS. These results reveal the capability of POT to act as a protective layer on LCS.

The SEM image of the POT coated LCS after the potentiodynamic polarization measurement in aqueous 3% NaCl is shown in Figure 10. It is seen that there is no apparent change in the surface morphology of the coating after the potentiodynamic polarization measurements. Indeed, the visual observation revealed no cracks in the coating and the coating remains strongly adherent to the LCS substrate. Thus, POT coating has strong adherence to the LCS substrate and it is resistant to the corrosion in aqueous 3% NaCl.

The outstanding corrosion protection offered by POT coating to LCS may be attributed to the fact that the deposited polymer is strongly adherent and uni-

formly covers the entire electrode surface as evident by the SEM. Furthermore, the delocalized π -electrons in this polymer facilitate its strong adsorption on the LCS surface, leading to the outstanding corrosion inhibition.

To investigate the influence of the coating thickness on the corrosion protection properties of the POT coatings, we have synthesized the coatings by 5, 10, 15, 20, and 25 cycles from -500 to $1,500$ mV at a scan rate of 20 mV/s and the potentiodynamic polarization resistance measurements were performed in an aqueous solution of 3% NaCl. It is found that the corrosion rate changes significantly (*cf.* Table I) when the deposition time (i.e., the number of cycles) is varied. The variation of the corrosion rate as a function of the number of cycles is shown in Figure 11. It is observed that the corrosion rate decreases with the increase in the number of cycles. The lowest corrosion rate is observed for the POT coating deposited with 25 cycles. Thus, the thick POT coatings appears to have outstanding corrosion properties. Thus, it seems that the thickness of the coating significantly affects the corrosion protection properties of the POT coatings.

It is interesting to observe that the absorbance values at 540 nm increase with an increase in the number of cycles used for the deposition of the coating as shown in Figure 11. This suggests that the PB form of POT provides better protection to LCS in aqueous 3% NaCl. This observation is in agreement with that reported by several researchers.²⁴

To further reveal the corrosion protection ability of the POT coating, we have studied the electrochemical behavior of the POT coated LCS electrode in a $0.1M$ aqueous solution of sodium tartrate (without *o*-toluidine). The CVs recorded for bare and POT coated LCS in the potential range between -500 and $1,500$ mV at

TABLE I
Potentiodynamic Polarization Measurement Results

Sample	E_{corr} (mV)	I_{corr} ($\mu\text{A}/\text{cm}^2$)	CR (mm/yr)
Bare LCS	-710	30.72	0.35
POT coated LCS 5 cycles	-469	2.51	0.03
POT coated LCS 10 cycles	-386	2.21	0.025
POT coated LCS 15 cycles	-384	1.67	0.019
POT coated LCS 20 cycles	-391	1.15	0.013
POT coated LCS 25 cycles	-376	0.65	0.007
POT removed LCS	-719	28.43	0.33
POT coated LCS (25 cycles) kept in air for 8 days at 25°C	-393	0.77	0.009

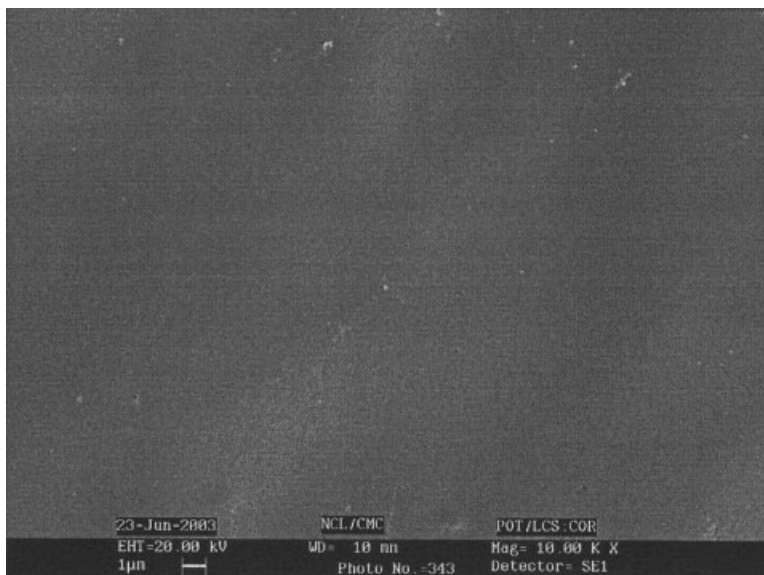


Figure 10 SEM of POT coating synthesized on LCS substrate under cyclic voltammetric conditions after potentiodynamic polarization measurement.

a scan rate of 20 mV/s in a 0.1M aqueous solution of sodium tartrate are shown in Figure 12. The first scan of the CV recorded for bare LCS substrate [Fig.12(a)] is similar to that shown in Figure 1(a). As discussed earlier, it indicates the dissolution of the LCS electrode surface. The first scan of the CV recorded for POT coated LCS [Fig.12(b)] is significantly different from

that for bare LCS. The anodic peak A and an oxidation wave B are not observed. The absence of the anodic peak A and the observation of negligibly small current densities at all potentials indicates that the dissolution of the underlying LCS substrate is inhibited due to the POT coating. Thus the "thick" POT coatings appear to have outstanding corrosion protection properties.

It is pointed out that the POT coating is soluble in DMSO solution, whereas the iron tartrate interphase is insoluble. The iron tartrate interphase remains as it is even after keeping it in DMSO solution for 30 min. As discussed earlier, the iron tartrate interphase formed during the early stages of the growth inhibits the dissolution of LCS. However, it does not prevail at the electrode surface and it seems that it undergoes dissolution and facilitates the ECP of *o*-toluidine. Further evidence in support of this was obtained by comparing the corrosion behavior of the POT removed LCS substrates with that of bare LCS. The POT coating was removed carefully by dissolving it in DMSO and the potentiodynamic polarization measurements were performed in the aqueous solution of 3% NaCl. The potentiodynamic polarization curves for the bare LCS and the POT removed LCS are shown in Figure 13. Interestingly, the E_{corr} and the corrosion rate for both the samples are very similar. This suggests that the passive iron tartrate interphase formed during the early stages of the growth does not remain at the electrode surface and the protection of the LCS is mainly due to the POT coating.

We have also performed the potentiodynamic polarization resistance measurements by using the POT coated (25 scan) LCS substrates after storing them in air at 25°C for 8 days and the corresponding polariza-

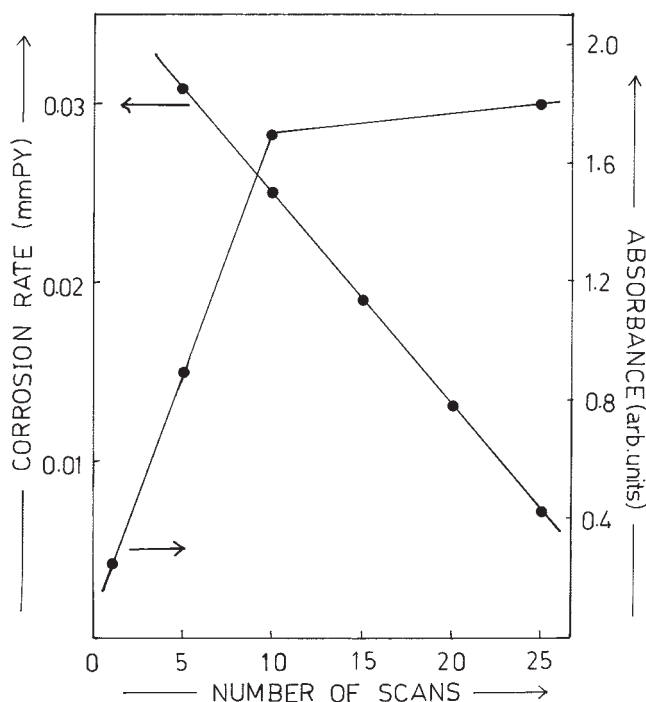


Figure 11 Variation of corrosion rate and absorbance values at 540 nm as a function of number of scans employed for synthesis.

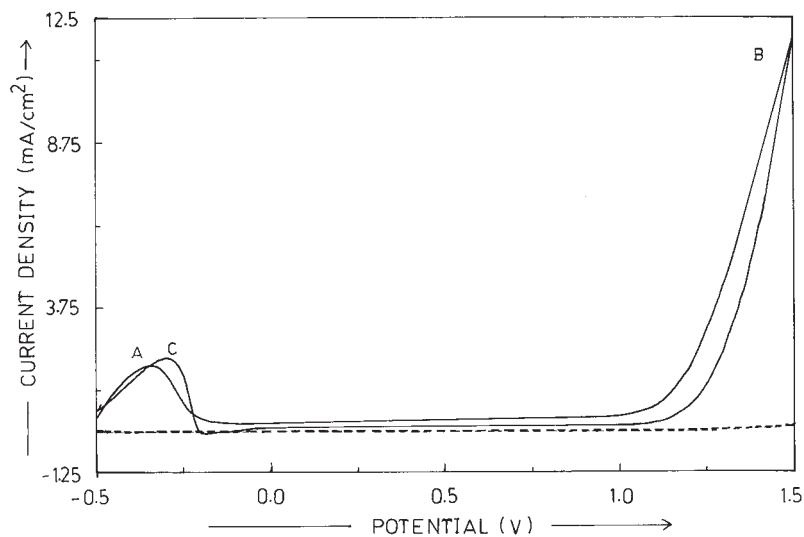


Figure 12 Cyclic voltammograms of (a) bare LCS and (b) POT coated LCS recorded in 0.1M sodium tartrate solution.

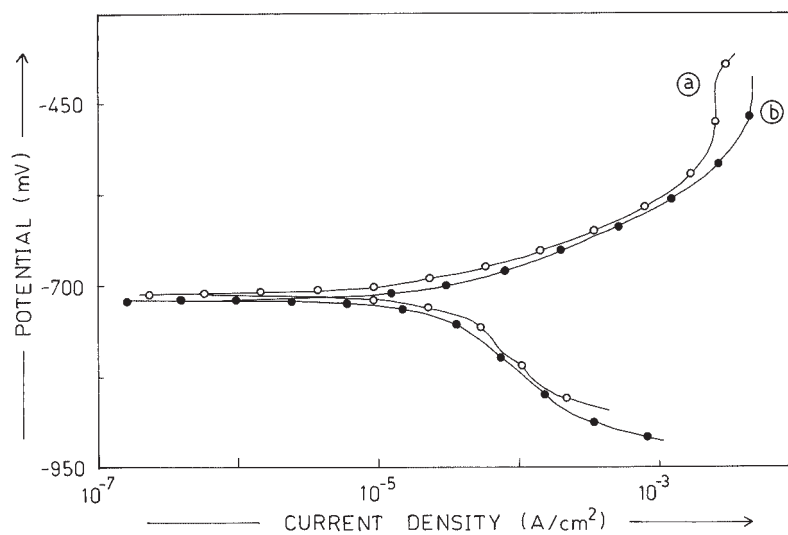


Figure 13 Potentiodynamic polarization curves for (a) bare LCS and (b) POT removed LCS recorded in aqueous 3% NaCl solution.

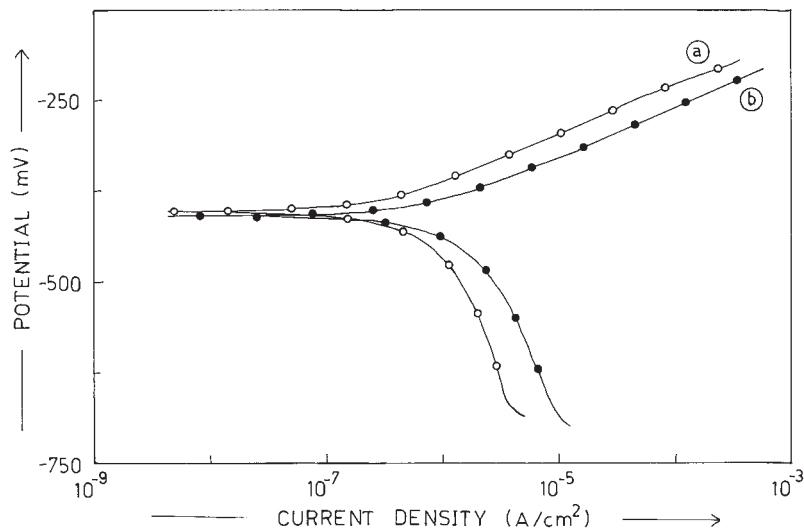


Figure 14 Potentiodynamic polarization curves for POT coated LCS (a) freshly prepared and (b) after storing in air for 7 days at 25°C recorded in aqueous 3% NaCl solution.

tion curve is shown in Figure 14(b). These curves clearly reveal that there is no indication of any substantial loss in corrosion protection properties of the POT coatings. Thus, the POT coating shows high chemical as well as physical stability because the coating keeps its adherence to LCS substrate even after the storage.

CONCLUSION

In summary, the following conclusions have been drawn from the present investigation:

- The ECP of *o*-toluidine in aqueous sodium tartrate solution results in the deposition of uniform and strongly adherent POT coatings on LCS substrates.
- The ECP process occurs without noticeable dissolution of LCS substrate.
- The result of the optical absorption spectroscopy depends on the thickness of the coating. It reveals the exclusive formation of the PB form in a thick coating, whereas the mixed phase of PB and ES forms is observed in thin coating.
- Potentiodynamic polarization studies reveal that the POT acts as a corrosion protective coating on LCS.
- The corrosion rate of POT coated (25 scan) LCS is found to be ~ 50 times lower than that observed for bare LCS.
- The PB form of POT is more effective for corrosion protection of LCS in a chloride environment.
- The corrosion protection properties of these coatings are retained even after storing them in air at 25°C for 8 days.
- This study clearly reveals that the POT coating has excellent corrosion protection properties and it can be considered to be potential coating material for corrosion protection of LCS in aqueous 3% NaCl.

Financial support from Defence Research and Development Organization (DRDO), India through DRDO/ISRO-PUNE University Interaction Cells, University of Pune, India is gratefully acknowledged. V.S. is thankful to North Maha-

rashtra University, Jalgaon, for awarding the research fellowship through the Chief Minister's fund.

References

1. Skotheim, T. A. Ed., Handbook of Conducting Polymers; Vols. I and II; Marcel Dekker: New York, 1986.
2. Salaneck, W. R.; Clark, D. T.; Samuelsen, E. J. Science and Applications of Conducting Polymers, Adam Hilger: Bristol, 1991.
3. Aldissi, M. Intrinsically Conducting Polymers: An Emerging Technology, Kluwer Academic Publishers: Dordrecht, The Netherlands, 1993.
4. Nalwa, H. S. Handbook of Organic Conductive Molecules and Polymers; Vols. 1-4; John Wiley and Sons Ltd.; New York, 1997.
5. Chandrasekhar, P. Conducting Polymers: Fundamentals and Applications; Kluwer Academic Publishers: Dordrecht, The Netherlands, 1999.
6. Scrosati, B. Application of Electroactive Polymers; Chapman and Hall: London, 1993.
7. Kilmartin, P. A.; Trier, L.; Wright, G. A. Synth Met 2002, 131, 99.
8. Araujo, W. S.; Margarit, I.C.P.; Ferreira, M.; Mattos, O. R.; Lima Neto, P. Electrochim Acta 2001, 46, 1307.
9. Nguyen Thi Le, H.; Garcia, B.; Deslouis, C.; Le Xuan, Q. Electrochim Acta 2001, 46, 4259.
10. Herrasti, P.; Ocon, P. Appl Surf Sci 2001, 172, 276.
11. DeBerry, D. W.; Viehback, A.; In Mccafferty, E.; Clayton, C. R.; Oudar, J. Eds.; The Electrochemical Society Softbound Proceedings Series; Electrochemical Society, Inc.: Pennington, NJ, 1984; p 308.
12. Beck, F.; Michaelis, R.; Schloten, F.; Zinger, B. Electrochim Acta 1994, 39(2), 229.
13. Mattoso, L. H. C.; Bilhotes, L. O. S. Synth Met 1992, 52, 171.
14. Mattoso, L. H. C.; Manohar, S. K.; MacDiarmid, A. G.; Epstein, A. J. Polymer Sci Part A: Polymer Chem 1995, 33, 1227.
15. Wankhede, M. G.; Koinkar, P. M.; More, M. A.; Patil, P. P.; Gangal, S. A. Adv Polym Tech 2002, 21, 33.
16. Electrochemistry and Corrosion: Overview and Techniques, Application Note CORR -4, EG and G, Princeton Applied Research: Oak Ridge, TN; p 8.
17. Bazzaoui, M.; Martins, L.; Bazzaoui, E. A.; Martins, J. I. Electrochim Acta 2002, 47, 2953.
18. Mengoli, G.; Musiani, M. M. Electrochim Acta 1986, 31, 201.
19. Tang, J.; Jing, X.; Wang, B.; Wang, F. Synth Met 1988, 24, 231.
20. Ohsaka, T.; Ohnuki, Y.; Oyama, N.; Katagiri, G.; Kamisako, K. J Electroanal Chem 1984, 161, 399.
21. Zheng, W. Y.; Levon, K.; Taka, T.; Laakso, J.; Osterholm, J. E.; Polym J 1996, 28, 412.
22. Shinde, Vandana; Patil, P. P. Mater Sci Technol (to appear).
23. Patil, S. Ph.D. Thesis; North Maharashtra University, Jalgaon, India, 2000.
24. Wei, Y.; Wang, J.; Jia, X.; Yeh, J. M.; Spellane, P. Polymer 1995, 36, 4535.